



Universitat de Lleida

Document downloaded from:

<http://hdl.handle.net/10459.1/62930>

The final publication is available at:

<https://doi.org/10.1016/j.renene.2018.02.018>

Copyright

cc-by-nc-nd, (c) Elsevier, 2018



Està subjecte a una llicència de [Reconeixement-NoComercial-SenseObraDerivada 4.0 de Creative Commons](https://creativecommons.org/licenses/by-nc-nd/4.0/)

Fluid-based spectrally selective filters for direct immersed PVT solar systems in building applications

D. Chemisana^{1,*}, E.F Fernandez², A. Riverola¹, A. Moreno¹

¹Applied Physics Section of the Environmental Science Department, University of Lleida, Jaume II 69, 25001 Lleida, Spain

²Centre for Advanced Studies on Energy and Environment (CEAEMA), University of Jaén, Las Lagunillas Campus, 23071 Jaén, Spain

*Corresponding author: daniel.chemisana@macs.udl.cat

Abstract

Liquid filters applied in hybrid photovoltaic-thermal (PVT) solar systems report potential benefits as they allow for selecting the wavelengths at which the solar cell operates with higher efficiency. Among the rest, low frequency photons are absorbed by the liquid, therefore not warming the cell up. In addition, direct immersion of photovoltaic cells in liquids enhances temperature control by cooling the cells under almost negligible contact resistance between the liquid and the cell. The characteristics of the liquids for direct immersed PVT application are described, defining an indicator (ideal filter window) to select the best liquid depending on the PV technology and the incident irradiance. Several liquids are assessed based on the required properties for the present application. As a conclusion, regarding optical, thermal, electrical and operational aspects, a mixture of deionized water and isopropyl alcohol results as proper candidate satisfying well all of them.

Keywords: Fluid-based filters; Direct immersion; Hybrid photovoltaic-thermal (PVT); Spectral selection; Dielectric liquids.

27 **List of symbols and abbreviations**

28	AM	air mass [-]
29	AOD (or τ)	aerosol optical thickness [-]
30	c-Si	crystalline silicon
31	C_e	specific heat [$J g^{-1} K^{-1}$]
32	CIGS	copper indium gallium diselenide
33	D	inner tube diameter [m]
34	DIW	deionized water
35	DMSO	dimethyl sulfoxide
36	d_s	total thickness of the cuvette [mm]
37	GaAs	gallium arsenide
38	GLY	glycerol
39	I_0	diode saturation current [A]
40	I_F	diode forward current [A]
41	I_R	diode reverse current [A]
42	IBA	isobutyl alcohol
43	IFW	ideal filter window
44	IPA	isopropyl alcohol
45	$J_{sc}(\lambda)$	spectral short-circuit current density [$A m^{-2} nm^{-1}$]
46	J_{sc}	short-circuit current density [$A m^{-2}$]
47	k	extinction coefficient [-]
48	L	pipe length [m]
49	n_D^{20} (or n)	refractive index at 20°C and 589 nm (sodium yellow doublet D-line) [-]
50	n^*	complex refractive index [-]
51	v	fluid velocity [m/s]
52	V	potential [V]
53	PW	precipitable water [cm]
54	Q	flow rate per collector aperture area [$l h^{-1} m^{-2}$]
55	Re	Reynolds number [-]
56	SR	spectral response [$A W^{-1}$]
57	T	temperature [K or °C]

58 **Greek symbols**

59	α	absorption coefficient [cm^{-1}], $\alpha = 4\pi k \lambda^{-1}$
60	ϵ_r	dielectric constant [-]
61	λ	wavelength [nm]
62	μ	dynamic viscosity [Pa s]
63	ρ	density [$kg m^{-3}$]

64

65 **1 Introduction**

66 Hybrid photovoltaic-thermal (PVT) solar collectors can be a high-efficient technology
67 able to cogenerate heat and electricity with global efficiencies around 70%, with
68 electrical efficiencies near 20% and thermal efficiencies higher than 50% [1]. One of the
69 main applications of such technologies is the building sector where both heat and
70 electricity are needed and 40% of the total energy consumption in Europe is registered
71 [2]. The on-site renewable energy production is the only solution to achieve buildings
72 with nearly-zero or zero energy consumption, and therefore, space limitations lead to
73 the necessity of efficient and space saving technologies such as PVT collectors. In this
74 regard, it has been demonstrated that 60% additional area is required for a separate solar
75 thermal collector and PV module to produce the same yield as a PVT liquid system [3].
76 On the other hand, direct immersed PVs have proved to enhance efficiency attending to
77 a reduction of the Fresnel losses with respect to a bare PV, a reduction of the surface
78 recombination losses [4] and a better temperature control by the reduction or
79 elimination of the thermal contact resistance at the interface between PVs and dissipater
80 [5]. Despite these notable benefits, direct immersed PVTs have to be further
81 investigated to completely understand their performances and key design parameters to
82 leverage their potential.

83 In order fill the gap in direct-immersed PVT collectors characteristics and to address the
84 goal of designing high-efficient PVT systems for applications in buildings, the present
85 research focuses on the investigation of several fluid-based optical filters for direct
86 immersion of the solar cells which aim at covering a double objective: (1) the filter
87 should adapt the incident spectrum to transmit photons at the photovoltaic cell
88 maximum spectral response bandwidth and absorb photons out of this zone; (2) the fluid
89 should remove the infrared photons emitted by the solar cell to prevent from problems

90 associated with overheating as efficiency reduction, thermal stress or dilatation of
91 materials, etc. First, the optical, electrical and thermal characteristics that a liquid filter
92 for PVT generation should achieve are discussed and stated. Later, a series of
93 experiments and calculations are conducted to categorize a set of candidate liquids
94 based on the requirements previously defined.

95 **2. Key characteristics of a liquid filter for direct immersed PVT collectors**

96 In the following subsections, the optical, electrical and thermal properties that a fluid-
97 based filter should meet are analyzed.

98 **2.1 Optical properties**

99 The optical properties studied are directly related to the optical constants involved in the
100 complex refractive index ($n^* = n + ik$). The refractive index, n , (real part), should
101 balance the refractive indexes of the module components in order to minimize Fresnel
102 losses. The imaginary part (the extinction coefficient, k) is analyzed, instead of the
103 directly related absorption coefficient (α), in terms of the spectral transmittance since
104 this is the most widely referred parameter.

105 The spectral transmittance requirements for the liquid filters should be in agreement
106 with two factors, namely: a) to transmit the maximum for optimizing the PV electrical
107 output and b) to absorb the maximum for optimizing the heat dissipation and
108 production.

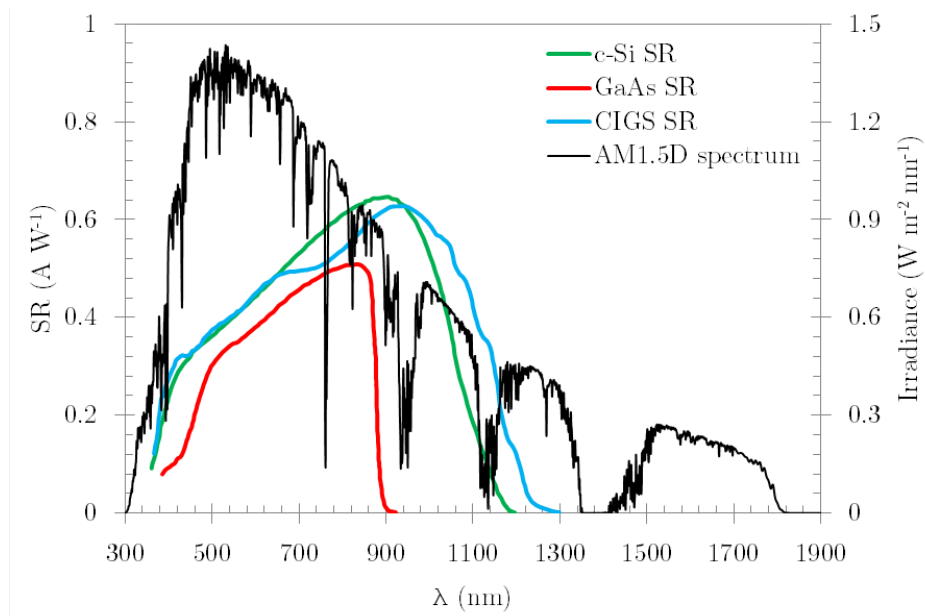
109 Regarding the electrical generation, some researchers define an ideal filter bandwidth
110 selection criterion based on the spectral response (SR) of the cell [6, 7]. For instance, in
111 [6] the criterion is to select the bandwidth at which the spectral response of the cell (c -
112 Si) is greater than 0.5 A/W. This criterion could be considered as a good first approach

113 when studying the zone where the liquid filter should transmit the maximum to optimize
114 the generation of the semiconductor device. However, it does not consider the solar
115 spectrum shape and its impact as a function of the specific SR of the device. A second
116 strategy is to define the appropriateness and behavior of the liquid filter relying on the
117 solar characteristics of the AM1.5 direct (D) reference spectrum [8]. Finally, some
118 authors analyze the performance of liquids considering both the SR and the solar
119 AM1.5D spectrum [9, 10]. Nevertheless, there is no study in the literature defining
120 explicitly the transmittance window the filter should match depending on the PV
121 technology and the particular incident solar spectrum. Concerning solar spectrum, only
122 the AM1.5D is referred as the most general while in the majority of the locations the
123 annual mean spectra differ considerably from the AM1.5D as the atmospheric
124 parameters are far from those included in the AM1.5D standard spectrum definition
125 [11].

126 A proper parameter to cope with the definition of the ideal filter for enhancing the PV
127 performance is the spectral short-circuit current density, $J_{sc}(\lambda)$, which is obtained by the
128 product of the SR of the PV technology and the spectral incident solar irradiance. Figure
129 1(a) shows the spectral responses of three characteristic PV cell technologies jointly
130 with the AM1.5D solar spectrum. From these data, the spectral short-circuit current
131 densities are calculated and plotted in Figure 1(b).

132

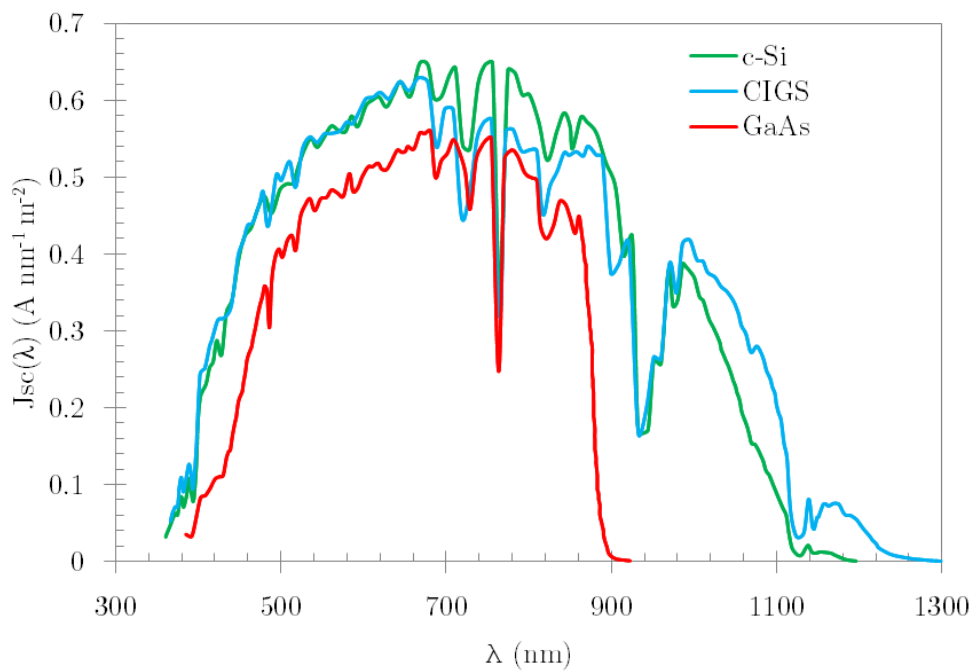
133 (a)



134

135

136 (b)



137

138 Figure 1. (a) AM1.5D standard spectrum and c-Si, CIGS and GaAs spectral responses;

139

(b) Spectral short-circuit current density of the three PV technologies.

140

141 From the spectral short-circuit current, it is defined the range of an ideal filter as the

142 minimum bandwidth which comprises at least the 75% of the short-circuit current

143 generated by the PV cell. The 75% value is selected as a compromise between the
 144 increase of short-circuit current density generation and the additional bandwidth needed
 145 to obtain such increment. The spectral short-circuit current density curves (Fig. 1(b))
 146 show a clear decrease in the generation at the tails, where the gain of generation per
 147 wavelength increment becomes very low. This condition could vary for different PV
 148 technologies and/or incident illumination conditions that would produce, for instance, a
 149 more constant spectral short-circuit current generation.

150 The criteria for the ideal liquid filter are indicated in Eq. (1). Subscripts i and f indicate
 151 the initial and final wavelengths where the PV cell generates current and subscripts a
 152 and b refer to the interval limits of the ideal filter window.

$$153 \quad \text{Ideal filter window (IFW) criteria} \left\{ \begin{array}{l} \frac{\int_{\lambda_a}^{\lambda_b} J_{SC}(\lambda) d\lambda}{\int_{\lambda_i}^{\lambda_f} J_{SC}(\lambda) d\lambda} \geq 0.75 \\ \min[\lambda_b - \lambda_a] \end{array} \right. \quad (1)$$

154 For the three photovoltaic technologies depicted in Figure 1, the spectral ranges
 155 fulfilling the stated conditions under AM1.5D spectrum are included in Table 1.

156 Table 1. Ideal filter window intervals and bandwidths for three PV technologies and
 157 under AM1.5D spectrum.

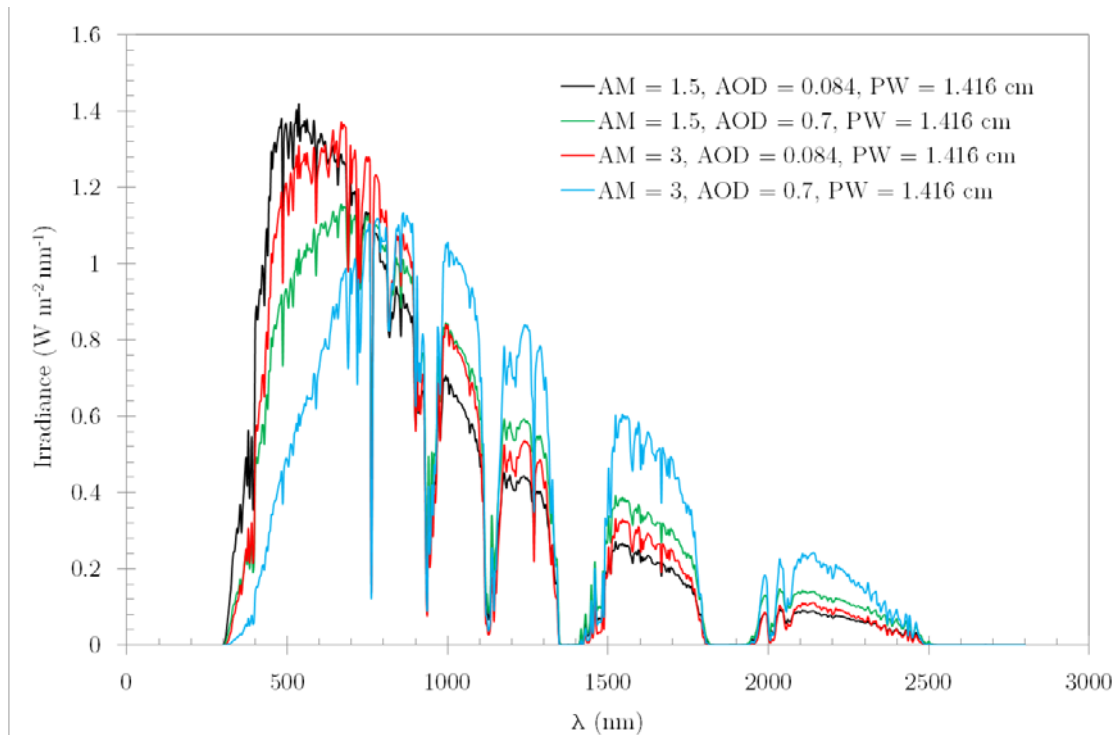
PV technology	$IFW_{AM1.5}$ (nm)	$\Delta\lambda$ (nm)
c-Si	422.4-893.3	470.9
CIGS	407.9-920.9	513.0
GaAs	477.5- 850.3	372.8

158
 159 In the following paragraphs the ideal filter window wavelength interval is assessed for
 160 annual mean spectra different from the AM1.5D standard reference spectrum. The
 161 calculated spectra aim at covering all the possible casuistic by considering the
 162 atmospheric parameter values that produce bigger changes in the spectrum. Also, since
 163 one of the main potential applications of liquid-based filters is for PVT concentrating

164 modules [5, 6, 8, 9], the direct irradiance spectra are only considered. Moreover, under
165 direct beam conditions, spectral changes due to atmospheric parameters variations are
166 more sensitive because diffuse irradiance does not interfere.

167 The atmospheric variables that mostly affect the solar spectrum characteristics are the
168 air mass (AM), aerosol optical depth (AOD or τ) and precipitable water (PW). AM is
169 defined as the distance, relative to the shortest (vertical) path length, that the sunrays
170 traverse through the atmosphere before impacting the Earth's surface. AOD
171 characterizes the radiative strength of aerosols (urban haze, smoke particles, desert dust,
172 sea salt, etc.) in the vertical direction. Finally, PW is the amount of condensed water
173 (expressed in cm) corresponding to the total water vapor contained in a vertical
174 atmospheric column above any location. The water vapor has strong absorption bands in
175 the near infrared, which directly impacts the spectrum. The explicit influence of these
176 atmospheric parameters on the spectrum is described in previous works for both the
177 direct and global spectral irradiance [12, 13]. As it was previously commented, the most
178 important atmospheric parameters that influence the spectrum shape are AM and AOD,
179 which lead to noteworthy attenuation effects on the Ultraviolet-Visible waveband, while
180 PW only modifies slightly the infrared portion. Figure 2 illustrates the spectral content
181 variation for the combination of parameters for which the spectrum is more sensitive.
182 The air mass annual mean of 3 represents a representative high value and the aerosol
183 optical depth of 0.7 indicates highly turbid conditions [12]. The reference AM1.5D
184 spectrum parameters are: AM = 1.5, AOD (at 500 nm) = 0.084 and PW = 1.416 cm. The
185 spectra are generated using the Simple Model of the Atmospheric Radiative Transfer of
186 Sunshine (SMARTS 2.9.5) [14]. The spectra are normalized to the same irradiance (the
187 AM1.5D one) in order to focus the discussion on the wavelengths effect on the PV cell

188 generation for the IFW definition and to better illustrate how the spectrum changes as a
189 function of the atmospheric parameters.



190

191 Figure 2. Generated spectra for several atmospheric parameters combinations.

192

193 Figure 3 plots the IFW interval limits for the spectra combinations. Looking at the c-Si
194 cell, the movement of the spectrum maximum to longer wavelengths due to the increase
195 of AM does not affect the IFW because even though the cell is more efficient for those
196 wavelengths the intensity of the spectrum is lower due to atmospheric absorption
197 around 700nm (case A). However, the more pronounced red-shift that occurs in the
198 cases B and C influences the widening of the IFW bandwidth and, specifically in the
199 case C there is a displacement of the IFW intervals to longer wavelengths. This
200 performance is analogous for the CIGS technology. On the contrary, the ideal filter
201 maximum transmittance bandwidth for GaAs cells is practically not sensitive to spectral
202 variations. This is associated to the narrower bandwidth where the cell is efficient. For
203 this reason the upper interval of the IFW does not move from around 850 nm and the

204 lower interval moves to slightly higher wavelengths caused by the red-shift mentioned
 205 above. Therefore, the IFW intervals should be defined depending on the location and its
 206 associated spectrum. It is worth mentioning that the analysis conducted here aims at
 207 demonstrating the variability of the IFW in terms of annual mean spectra, but for the
 208 exact calculation of the IFW for a specific location it should be determined considering
 209 the annual spectral variations and selecting the interval which maximizes power output.

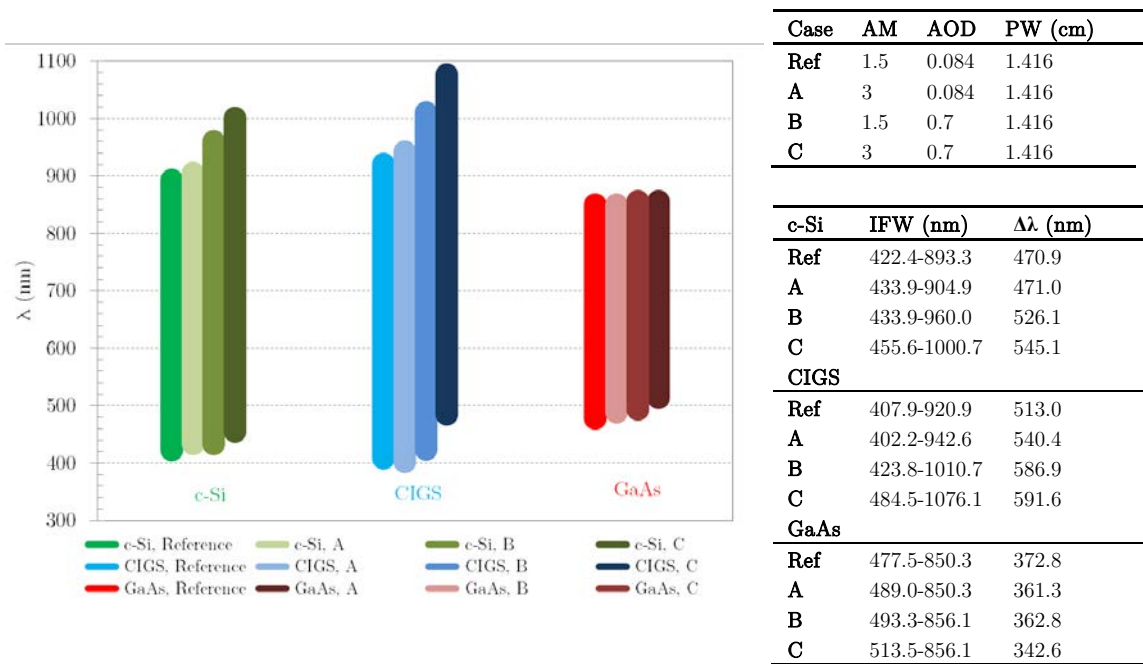


Figure 3. IFW intervals for different PV technologies and incident spectra.

210

211 On the other hand, the transmittance of the filter should be minimal from the thermal
 212 point of view for the rest of the wavelengths which are not appropriate for electrical
 213 generation. Certainly, this is hardly achievable since two clear areas are identified:
 214 irradiances of photons with shorter wavelengths than the minimum of the IFW and
 215 irradiances of longer wavelengths than the maximum of the IFW. Concerning the short
 216 wavelengths, these are not problematic at all as in most of the cases the glazing element
 217 utilized in the PVT modules is soda lime glass which, depending on the silica content,
 218 does not transmit wavelengths shorter than 300-350 nm. In addition, even with less

219 efficiency and warming the solar cell up by thermalization effect those more energetic
220 photons contribute in pumping electrons. Finally, this bandwidth around 400 nm fits
221 very well the absorption wavelengths of several luminescent dyes which re-emit at
222 wavelengths included in the IFW interval [15, 16]. From the above mentioned, the
223 liquid filters should present minimum transmittances for bandwidths above the upper
224 limit of the IFWs.

225 **2.2 Electrical properties**

226 The main electrical property that a liquid for direct immersion has to fulfill is to be
227 dielectric. In addition, some authors associate the dielectric to an electrical performance
228 increase of the PV cell due to a positive effect originated by the adhesion of the liquid
229 dipole to the cell:

230 a) Ugumory and Ikeya [17] found that the photocurrent of solar cells operated in liquid
231 increases with the increase in the permanent dielectric moment (rather than the
232 dielectric constant) of liquid molecules. This increase in photocurrent was attributed to a
233 possible adsorption of the polarizable molecules which can reduce the surface
234 recombination current. In addition to the reduction of surface recombination effect, they
235 speculated that band bending at the surface could cause an increase in the
236 photoconductance, but they indicated that it was not possible to propose the definitive
237 mechanism for that.

238 b) Abrahamyan *et al.* [4] reported that a dielectric liquid thin-film can increase the
239 efficiency of common silicon solar cells by 40-60%, considering that the adhesion of
240 the liquid dipoles to the cell surface can result in lower surface recombination velocity
241 and lower light reflection. From the studied liquids, those experimenting higher increase
242 in short-circuit current and open-circuit voltage were acetone and glycerin. They

243 analyzed the electric effect in absence of light to eliminate reflection issues with and
244 without glycerin. The increase of short-circuit current, open-circuit potential and
245 efficiency was attributed to several factors: an increase in the barrier height of pn
246 junction, a decrease in the velocity of the surface recombination followed by an increase
247 in the factor of separation of charge carriers generated by light as well as a decrease in a
248 part of the reflected radiation. Moreover, they noticed that the increase of the thickness
249 of the liquid layer over the cells promotes the wetting and the adsorption phenomena,
250 but on the contrary the higher the thickness the higher the absorption. As a conclusion,
251 there should be an optimum thickness depending on the dielectric utilized.

252 c) Wang *et al.* [18] performed some tests and described a possible mechanism for cell
253 performance increase when immersed in a liquid. The adhered dipoles at the cell
254 surfaces, both front and back, originate electric fields with identical directions to the
255 built-in electric field in the cell. These electric fields at both surfaces can suppress the
256 surface recombination. However, the electric fields could also cause electric leakage,
257 which could result in a decrease of the shunt resistance. They differentiated between
258 non-polar and polar liquids, that present different permanent electric moment and in
259 consequence the electric fields formed vary their intensities depending on the liquid
260 molecule type. From the liquids tested (tap water, ethanol and silicone oil), they
261 selected the non-dipolar one as the best candidate (silicone oil).

262 d) Han *et al.* [4, 19] reported that the increase in the concentration of electrons in the n-
263 layer that is moistened with a liquid leads to a decrease in the saturation current
264 (proportional to the surface recombination reduction). They observed that the dark
265 current decreases more for polar liquids such as deionized water or isopropyl alcohol,
266 and less for non-polar liquids (dimethyl silicon oil and ethyl acetate).

267 **2.3 Thermal properties**

268 The thermal properties that make a liquid adequate for PVT modules are high specific
269 heat and high thermal conductivity to maximize thermal exchange and low coefficient
270 of expansion to prevent the increase of pressure inside the hydraulic circuit when
271 temperature increases. Also, the liquid should present an appropriate range of
272 temperatures between melting and boiling points so that real operational conditions are
273 well covered.

274 Direct liquid-immersion active cooling eliminates the thermal contact resistance at the
275 interface between PVs and dissipater. The contact thermal resistance is moved to the
276 boundary layer between the bulk liquid and the cell. In addition, it provides the
277 opportunity to cool the cells at both surfaces, top and rear, and not to be limited to the
278 back one as in the conventional coolers [5]. The thermal advantage of liquid immersion
279 cooling is more important than the increase in the electrical performance with the
280 dielectric. With the same flow rate (1.1 l/s) and inlet temperature (298K), deionized
281 water as coolant can make the operating temperature of the module 20°C lower than that
282 of isopropyl alcohol [5].

283 A very important aspect in an active PVT system is related to the power needed for
284 cooling-fluid pumping. In this direction, it is essential to maximize the liquid density
285 and to minimize the viscosity, so as the system can maximize the heat removal with low
286 pressure losses [20].

287 **3. Analysis of possible dielectric liquids candidates for spectral selection in PVT** 288 **collectors**

289 A set of dielectric liquids have been selected to study their performances based on the
290 optical, thermal and electrical characteristics described in section 2. The candidates are:

291 deionized water (DIW), isopropyl alcohol (IPA), isobutyl alcohol (IBA), dimethyl
 292 sulfoxide (DMSO), Glycerol (GLY) and some mixtures under different volumetric
 293 fractions (IPA / GLY, IPA / DIW, DMSO / DIW and DMSO / IPA). DIW is chosen
 294 because, even it may oxidize the metallic components under direct contact, it presents
 295 the best properties concerning the thermal and electrical desired characteristics (highest
 296 specific heat, thermal conductivity and the lowest electrical conductivity). IPA and IBA
 297 register a good range of operating temperatures between melting and boiling points, not
 298 only to work as pure substances but also to be a good mixture molecule to prevent the
 299 PVT module from freezing. GLY is the liquid for which the best electrical performance
 300 increase has been reported in the literature [4]. DMSO is the molecule with the second
 301 highest dielectric constant (48.9), it also presents high density, low viscosity and
 302 medium specific heat coefficient that make it appropriate from the thermal point of
 303 view. In Table 2 the different properties of the pure substances are shown. An additional
 304 column has been included regarding health toxicity in agreement with NFPA 704
 305 standard health code [21]. This ranges from 0 (no health hazard) to 4 (could cause death
 306 or major residual injury).

307 Table 2. Characteristics of the dielectric liquids. Physical properties are at 20°C except
 308 those indicating a specific temperature.

Liquid	ϵ_r	n_D^{20}	C_e (J g ⁻¹ K ⁻¹)	ρ (kg m ⁻³)	μ (mPa s ⁻¹)	[T _{melting} -T _{boiling}](°C)	Health code
DIW	80.2	1.330	4.18	1000	1.0	[0-100]	0
IPA	18.6	1.376	2.60	785	2.4	[-89-82.6]	1
IBA	15.8	1.396	2.30	802.5	3.9	[-108-107.9]	1
	(25°C)						
GLY	42.5	1.475	2.20	1100	1553	[17.8-290]	0
DMSO	48.9	1.478	1.96	1260	2.7	[19-189]	1

309

310

311

312 **3.1 Optical performance**

313 In the case of a direct immersed PVT system, the module configuration over the PV
314 cells presents two layers: the dielectric liquid and the transparent top casing that allows
315 transmitting the incident light and confines the liquid in the cavity. Attending to this
316 structure, the optical performance will be better when the refractive indexes of the
317 materials of the slab will be the most similar possible regarding Fresnel losses.
318 Considering that the most usual antireflection single layer is made of silicon nitride with
319 a refractive index around 2 and the transparent top layer could be either of polymeric
320 materials or glass with refractive indexes surrounding 1.5, the best liquids are those
321 achieving refractive indexes closer to the range (1.5-2). Based on this fact, the best
322 candidate would be DMSO and the worst DIW. Table 3 describes the Fresnel losses in
323 terms of the power loss at the PV cell level for the liquid candidates and under the slab
324 scheme mentioned (considering silicon nitride refractive index) at normal incidence. It
325 is assumed that at the n_D wavelength (589 nm) the extinction coefficient of the liquids is
326 negligible. It can be appreciated that the power loss is almost three times lower in the
327 case of DMSO than in the empty cavity, but at the same time the maximum difference
328 between liquids is small (around 2%).

329 Table 3. Fresnel power losses of the different liquids.

Dielectric liquid	Power loss (%)
No liquid in the cavity	18.1
DIW	8.22
IPA	7.46
IBA	7.16
GLY	6.20
DMSO	6.17

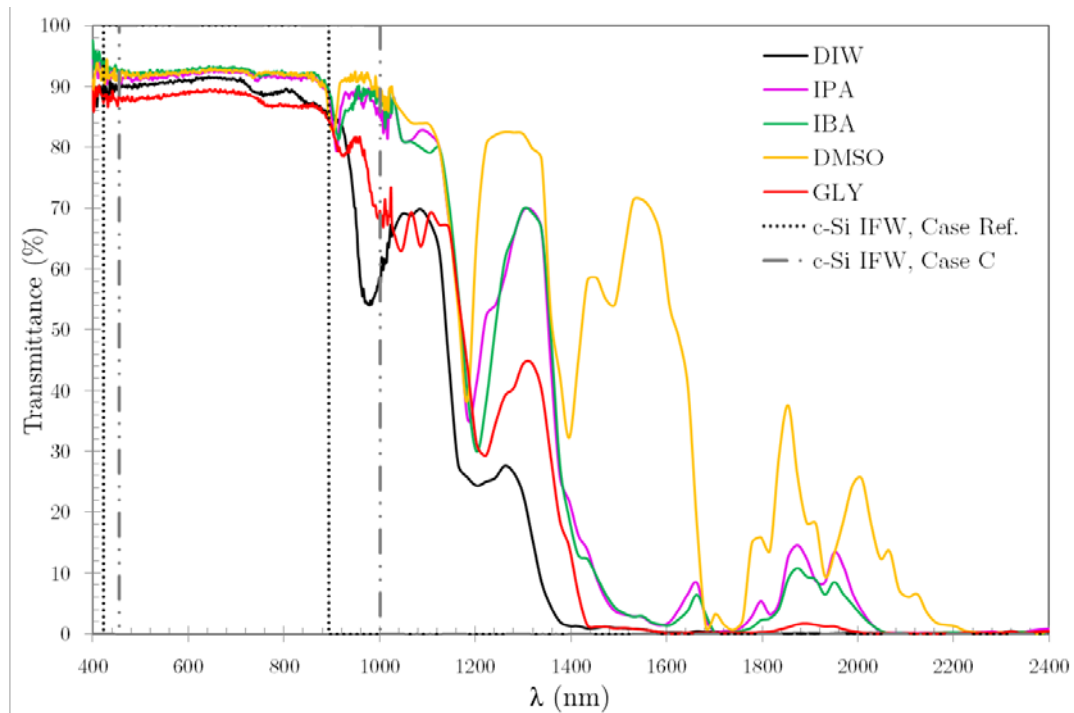
330

331 Concerning the transmittance of the liquids, it has been measured with an Ocean Optics
332 UV-VIS-NIR spectrometer utilizing a 10 mm light path optical glass cuvettes. The
333 range of the spectrometer (350-2500 nm) encompasses the 98.2% of the energy
334 comprised in the AM1.5D spectrum. It is assumed that no interference is produced as
335 the bandwidth ($\Delta\lambda$) used is 0.5 nm and the thickness of the three-slab system for the 10
336 mm cuvette (walls of 1 mm thick) is 12 mm (d_s). Therefore, for the worst case ($n = 1.33$
337 and $\lambda=2500$ nm), the incoherent superposition condition is met [22]:

$$d_s > \frac{\lambda^2}{2\pi n \Delta\lambda} \quad (2)$$

338 In Figure 4, the pure substances transmittances measured along with the IFW intervals
339 are included. The IFWs indicated correspond to the reference AM1.5D case and to case
340 C (AM = 3 and AOD = 0.7) for c-Si (for the other two PV technologies the analysis
341 would be analogous). In terms of the PV receiver, under the reference spectrum it can
342 be seen that all the substances behave adequately at maximum transmittances; however,
343 in the case C spectrum, the upper interval of the IFW moves to higher wavelengths into
344 a lower transmittance zone for the DIW and GLY. The rest of the liquids keep high their
345 transmittances. On the other hand, regarding the thermal performance of the PVT
346 collector, the transmittance should be minimal for longer wavelengths than the upper
347 limit of the IFW. GLY and DIW are the two liquids that clearly best suit this condition
348 for both IFWs. Since there is no coincidence under the most demanding IFW conditions
349 in the thermal and electrical requirements for the set of liquids, a series of mixtures were
350 prepared to try to decrease the transmittance above the upper IFW limits and to try to
351 increase the transmittance of GLY and DIW so that case C conditions are met. It should
352 be highlighted that the case C spectrum considered presents high values of AOD and
353 AM, but concerning the AM much higher values are observed during a day at the first

354 and last hours. Therefore, similar spectra to the one considered here with the red-shift
355 observed occur in all the places at certain moments of the day.



356

357

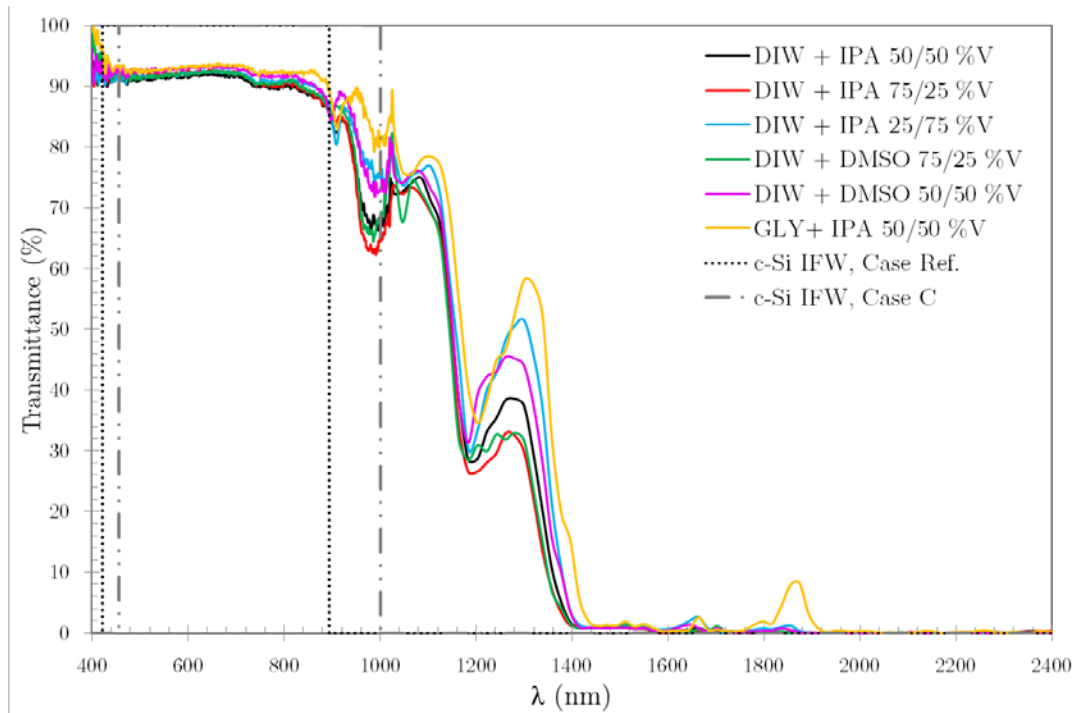
Figure 4. Spectral transmittances and IFW ranges for c-Si.

358 Figure 5 depicts the liquid mixtures transmittance spectra of those liquids selected based
359 on the previous transmittances obtained and conditioned to miscibility between them.

360 The criterion of mixing was to obtain the maximum transmittance in the IFW range and
361 the minimum transmittance above it. The two mixtures that best match the criterion are

362 DIW + DMSO and DIW + IPA as they balance the maximum and minimum
363 transmittance levels required for the PVT generation (%V indicates volumetric

364 proportions).



365

366

Figure 5. Liquid mixtures spectral transmittances and IFW ranges for c-Si.

367

3.2 Electrical performance

368

The dielectric liquids effect on the PV cell performance is analyzed by testing a batch of

369

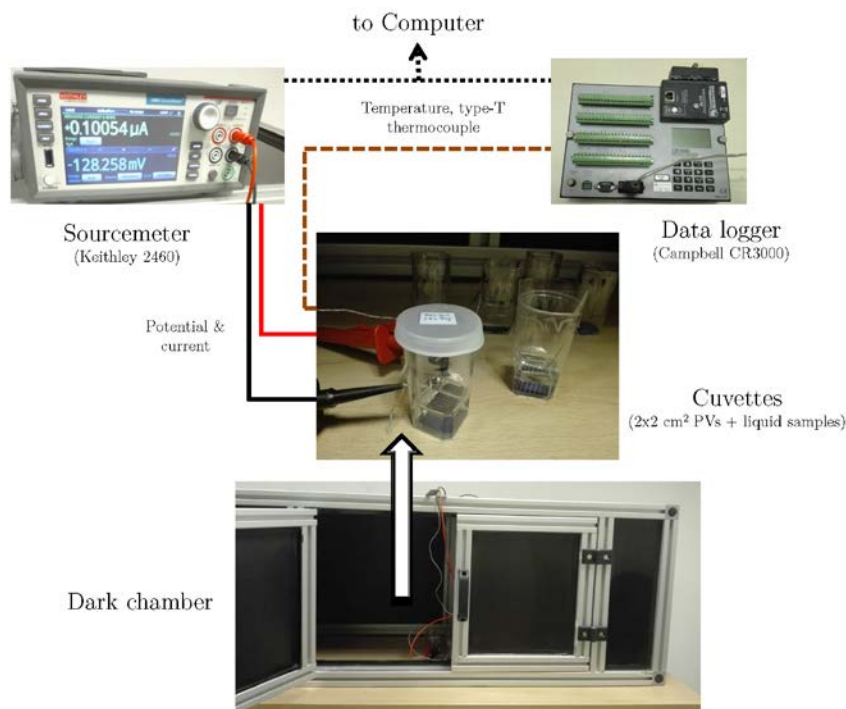
2x2 cm² solar cells immersed in 10 mm of the different liquids assessed inside a series

370

of cuvettes with a Keithley 2460 sourcemeter. In Figure 6, the experimental set-up

371

scheme is depicted.



372

373

Figure 6. Scheme of the electrical characterization experimental set-up.

374

Dark IV curves measurements before and after the cell immersion are conducted under

375

dark conditions to eliminate Fresnel losses and to directly identify if the dielectric

376

liquids affect the cell performance through the diode current. In the diode equation, the

377

saturation current (I_0) is referred as a direct indicator of the recombination phenomena,

378

but it shows a strong dependence on the temperature effects [23]. Therefore, no

379

temperature variations should be ensured to attribute the possible variations to changes

380

in the recombination rates associated to I_0 . A T-type high accuracy thermocouple is

381

attached at the back of the cells to perform the IV curve measurements at the same

382

temperature and few sampling points are applied to acquire the curve the fastest

383

possible. A small error is assumed since the measured temperature does not correspond

384

to the pn junction, even though the thermocouples are accurate, an error of 0.4 % is

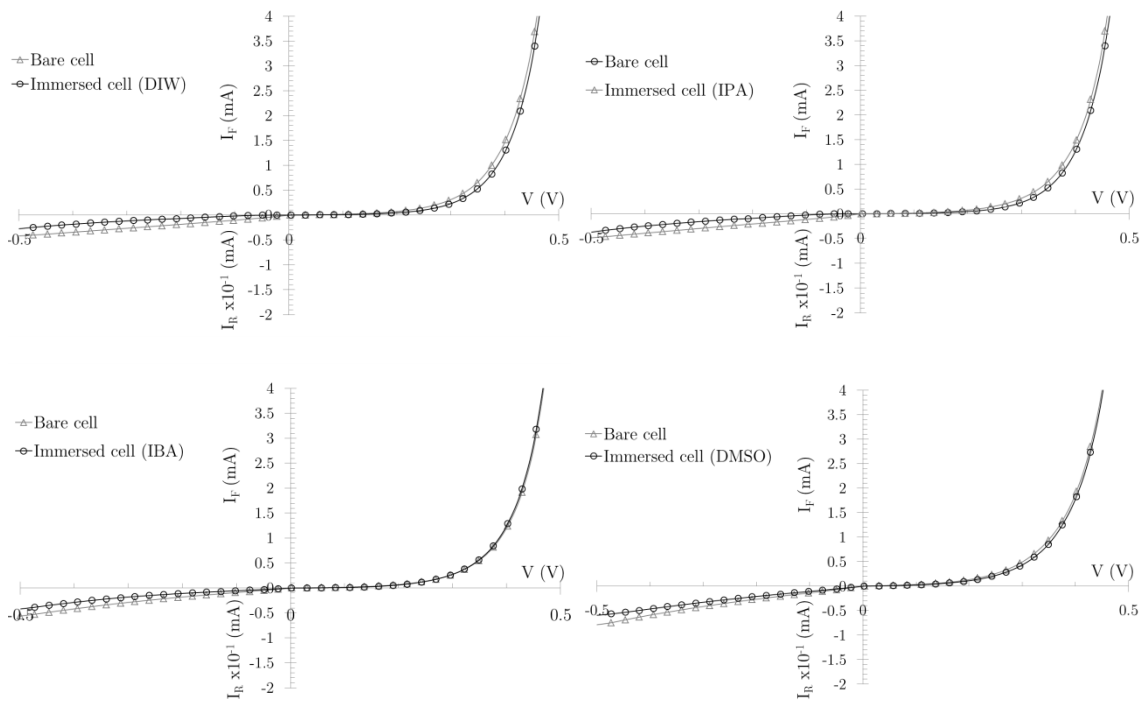
385

associated and the IV tracing is performed fast but around 2 seconds are needed. In

386

Figure 7, some of the measurements for the pure liquids are plotted, indicating that the

387 diode reverse current (I_R) decreases slightly when the cells are immersed in the different
 388 dielectric liquids. The shift of the diode current for a forward voltage bias (I_F) is very
 389 small for DIW and IPA and negligible for IBA and DMSO. This effect is in agreement
 390 with what has been reported by other authors [3, 4, 17-19], but it is necessary to point
 391 out that the positive effect observed is marginal in comparison with the performance
 392 increase due to Fresnel losses reduction or temperature control from the cells by the
 393 direct contact with the liquid. Since PV cells have experienced a continuous evolution
 394 to enhance performance, the passivation layers and techniques, among others, have been
 395 considerable improved. For this reason, the electrical performance increase produced by
 396 the dielectric liquids effect is small in comparison with that reported in 2002 by
 397 Abrahamyan *et al.* [4].



398

399

400 Figure 7. Characteristic dark IV curves. Temperatures of the measurements: DIW =
 401 22.45°C, IPA = 22.77°C, IBA = 23.07°C, DMSO = 20.47°C.

402

403

404 **3.3 Thermal performance**

405 The heat extraction capacity of the dielectric liquid in a PVT collector not only depends
406 on the liquid properties but also on the geometry and characteristics of the dissipation
407 scheme. Regarding the fraction of the incident irradiance that the liquid filter directly
408 absorbs, it can be derived from the irradiance fraction that is transmitted with respect to
409 the incident one. Considering the interval from 1000nm to 2500 nm, the percentages
410 transmitted by the pure substances calculated by the Fresnel equations and for
411 unpolarized light are included in Table 4. DMSO transmits an important percentage of
412 25% of the incident irradiance that only warms the PV cell up, which positions it as a
413 not good candidate from the thermal point of view. The rest of liquids achieve a quite
414 reasonable values ranging from 1 to 5%.

415 Table 4. Percentage of irradiance in the range (1000-2500) nm that is not absorbed by
416 the dielectric liquids.

Dielectric liquid	Irradiance transmitted (%), range (1000-2500) nm
DIW	1.15
IPA	5.01
IBA	4.43
DMSO	25.7
GLY	2.07

417

418 In concern to the rest of properties of the liquid as heat transfer fluid, a simple analysis
419 to estimate the pumping power necessary for a 1 m² aperture area flat-plate collector is
420 conducted based on the fluid properties of Table 2 and by considering the assumptions
421 defined in Table 5. Only primary pressure losses in the hydraulic circuit are included in
422 the calculations as the objective is to qualify the liquids independently of the collector
423 geometry.

424

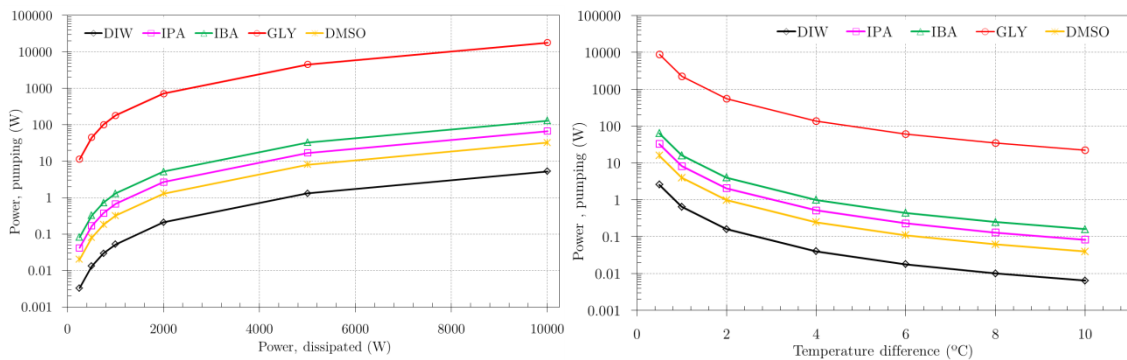
425

426 Table 5. Assumptions for the pumping power calculation. Re is the Reynolds number.

Inner pipe diameter , D (m)	0.01
Pipe length, L (m)	11
Flow rate, Q (l/h/m ²)	70
Velocity, v (m/s)	0.25
Primary pressure losses, ΔP (Pa)	$\Delta P = \frac{64Lv^2}{2ReD}$
Pumping power, (W)	Power = QΔP

427

428 In Figure 8, two sensitivity analyses are included: the first (Figure 8, left) shows the
 429 power necessary to pump the liquid keeping the temperature difference between the
 430 inlet and outlet at 7°C and for different dissipated powers; the second (Figure 8, right)
 431 maintains the removed power level at 500 W/m² while temperature raise varies from 1
 432 to 10°C. From both graphs it can be appreciated a clear change in the pumping
 433 requirements depending on the liquid. The most demanding is GLY, attending to its
 434 very high viscosity (even to be non-Newtonian liquid the viscosity value is considered
 435 not to vary). Conversely, the best liquid is DIW. In the middle region, DMSO, IPA and
 436 IBA appear. From these three, DMSO is the one achieving less pressure losses.



437

438 Figure 8. Pumping power (logarithmic scale) vs. dissipated power (left) and temperature
 439 difference (right).

440

441

442 **3.4 Operational properties**

443 In general, the changes in the spectral properties with time are only marginal for all the
444 dielectric liquids if they are not operating at temperatures above 80°C [6]. Nevertheless,
445 some affectations are reported in the literature. GLY become yellowish with time [24].
446 Deionized water, and polar liquids in general, could oxidize metallic components (tin,
447 silver and copper mainly in the electrical contacts and soldering), but the emitter is not
448 affected [5]. IPA is very stable for immersion [5, 7]. Alcohols in general may degrade
449 polymeric materials, including many types of sealants. The assessed alcohols do not
450 present problems with the working temperatures as they boil above 80°C. Nonetheless,
451 the rest of liquids melting points are at temperatures equal or greater than 0°C which
452 may cause freezing depending on the ambient temperatures of the location. For
453 European climates, in all the cases, it would be recommended to mix them with alcohols
454 in different fractions in order to reduce the freezing temperature depending on the
455 minimum temperatures at each specific the place. Finally, it is important to mention that
456 all the tested liquids are not dangerous from the health point of view.

457 **4 Summary and conclusions**

458 The use of liquid-based filters to spectrally select the incident irradiance in a direct
459 immersed photovoltaic-thermal module reports several benefits. These are based on the
460 possibility of selecting the photons that are most efficiently converted into electricity by
461 the PV cell to be transmitted and the photons out of this range to be absorbed by the
462 liquid to prevent from overheating.

463 Optical, electrical and thermal characteristics of the dielectric liquids have been
464 analyzed based on the state-of-the-art. The most important issues are:

- 465 • The liquids have to be highly transparent at the region where the solar cells are
466 more efficient.
- 467 • The refractive index of the liquids should be higher than the one of the air since
468 this produces a reduction in the Fresnel losses.
- 469 • The adsorption of the liquid dipoles at the front and rear surface of the cell may
470 improve the cell performance.
- 471 • The direct thermal contact between the cell and the liquid enhances heat
472 dissipation.

473 An ideal filter window indicator has been defined to identify the bandwidth at which the
474 filter should transmit the maximum and out of it should absorb the maximum. The
475 parameter takes into account the spectral response of the photovoltaic technology and
476 the incident spectrum as both are quite irregular in shape. In the case of the spectrum,
477 possible variations of its morphology due to atmospheric parameters variability
478 throughout the day and depending on the placement have also been discussed. The ideal
479 filter window and therefore, the requirements for the liquid filter to be used vary
480 considerably depending on atmospheric parameters variation (air mass index and
481 aerosol optical thickness are the parameters which most influence the spectrum).

482 A series of dielectric liquids candidates have been selected based on their optical,
483 thermal and electrical adequateness for the present application. The liquids have been
484 studied optically, thermally and electrically to state their advantages and disadvantages
485 for a PVT direct immersed solar module. Moreover, operational features have been
486 considered as freezing temperatures, stability, degradation of components, etc. Table 6
487 sums up the obtained results regarding the different aspects analyzed. The electrical
488 characteristics are not included as all the liquids respond satisfactory and not
489 substantially different.

490 Table 6. Summary of the results.

Liquid	Optical characteristics	Thermal characteristics	Operational characteristics
DIW	-high transparency at VIS bandwidth -refractive index low in comparison to the glass and ARC ones (Fresnel losses) -regarding PV performance, absorbs from 900nm on diminishing photons available.	-the best performance as heat extraction liquid	-possible oxidation of metallic components -need of mixing to avoid freezing
IPA	- high transparency at VIS bandwidth -refractive index close to those of glass and ARC but lower than the GLY and DMSO ones	-good heat extraction liquid	-may degrade polymers
IBA	-high transparency at VIS bandwidth -refractive index close to those of glass and ARC but lower than the GLY and DMSO ones	-good heat extraction liquid	-not miscible with DIW, GLY -may degrade polymers
GLY	- high transparency at VIS bandwidth -refractive index close to the glass, few Fresnel losses	-the worst performance as heat extraction liquid	-need of mixing to avoid freezing -need of mixing to reduce viscosity -possible yellowing
DMSO	-high transparency at VIS bandwidth -refractive index close to the glass, few Fresnel losses	-good heat extraction liquid -does not absorb an important part of the infrared photons that are not converted by the PV cell (25%)	-need of mixing to avoid freezing

491

492 From the obtained results, it can be concluded that proper candidates for PVT direct
 493 immersed modules would be some mixtures achieving: adequate melting points to avoid
 494 freezing, high transmittance for the bandwidth fixed based on the IFW criteria, high
 495 absorbance for photons above the upper interval of the IFW and good thermal
 496 characteristics to remove heat with the highest efficiency and lowest pumping power
 497 necessary. As a result, two liquids have been identified as optimal: a mixture of
 498 deionized water with isopropyl alcohol and a mixture of deionized water with dimethyl
 499 sulfoxide. The last may not properly work in cold climates as the freezing temperature
 500 is above 0°C.

501 **Acknowledgements**

502 The authors would like to thank "Ministerio de Economía y Competitividad" of Spain
503 for the funding (grant references ENE2013- 48325-R and ENE2016-81040-R).

504 **References**

505 [1] Al-Waeli, A.H.A., Sopian, K., Kazem, H.A. & Chaichan, M.T. 2017,
506 "Photovoltaic/Thermal (PV/T) systems: Status and future prospects", *Renewable and*
507 *Sustainable Energy Reviews*, vol. 77, pp. 109-130.

508 [2] European Parliament. Directive 2010/31/EU of the European Parliament and of the
509 Council of 19 May 2010 on the energy performance of buildings, 2010.

510 [3] da Silva, R.M., Fernandes, J.L.M. 2010, "Hybrid photovoltaic/thermal (PV/T) solar
511 systems simulation with Simulink/Matlab", *Solar Energy*, 84, 1985-1996.

512 [4] Abrahamyan, Y.A., Serago, V.I., Aroutiounian, V.M., Anisimova, I.D., Stafeev,
513 V.I., Karamian, G.G., Martoyan, G.A., Mouradyan, A.A. The efficiency of solar cells
514 immersed in liquid dielectrics. *Sol. Energy Mater. Sol. Cells* 2002, 73, 367–375.

515 [5] Han, X., Wang, Y. & Zhu, L. 2011, "Electrical and thermal performance of silicon
516 concentrator solar cells immersed in dielectric liquids", *Applied Energy*, vol. 88, no. 12,
517 pp. 4481-4489.

518 [6] Looser, R., Vivar, M. & Everett, V. Spectral characterisation and long-term
519 performance analysis of various commercial Heat Transfer Fluids (HTF) as Direct-
520 Absorption Filters for CPV-T beam-splitting applications. *Applied Energy* 2014, vol.
521 113, pp. 1496-1511.

522 [7] Taylor, R. A., Otanicar, T., Rosengarten, G. Nanofluid-Based Optical Filter
523 Optimization for PV/T Systems. *Light Sci. Appl.* 2012, 1, e34.

524 [8] Han, X., Wang, Y., Zhu, L., Xiang, H. & Zhang, H. 2012, "Mechanism study of the
525 electrical performance change of silicon concentrator solar cells immersed in de-ionized
526 water", *Energy Conversion and Management*, vol. 53, no. 1, pp. 1-10.

527 [9] Han, X., Wang, Y., Zhu, L., Xiang, H. & Zhang, H. 2011, "Reliability assessment of
528 silicone coated silicon concentrator solar cells by accelerated aging tests for immersing
529 in de-ionized water", *Solar Energy*, vol. 85, no. 11, pp. 2781-2788.

530 [10] Al-Shohani, W.A.M., Sabouri, A., Al-Dadah, R., Mahmoud, S. & Butt, H. 2016,
531 "Experimental investigation of an optical water filter for Photovoltaic/Thermal
532 conversion module", *Energy Conversion and Management*, vol. 111, pp. 431-442.

- 533 [11] ASTM, 2004. G173-03 Standard tables for reference solar spectral irradiances:
534 direct normal and hemispherical on 37° tilted surface. Book of Standards Volume:
535 14.04, American Society for Testing and Materials: West Conshohocken, PA.
- 536 [12] Vossier, A., Riverola, A., Chemisana, D., Dollet, A. & Gueymard, C.A. 2017, "Is
537 conversion efficiency still relevant to qualify advanced multi-junction solar cells?",
538 Progress in Photovoltaics: Research and Applications, vol. 25, no. 3, pp. 242-254.
- 539 [13] Fernández, E.F., Soria-Moya, A., Almonacid, F. & Aguilera, J. 2016,
540 "Comparative assessment of the spectral impact on the energy yield of high
541 concentrator and conventional photovoltaic technology", Solar Energy Materials and
542 Solar Cells, vol. 147, pp. 185-197.
- 543 [14] Gueymard CA. Parameterized transmittance model for direct beam and circumsolar
544 spectral irradiance. Solar Energy 2001; 71(5): 325–346.
- 545 [15] Aste, N., Tagliabue, L.C., Del Pero, C., Testa, D., Fusco, R. 2015, "Performance
546 analysis of a large-area luminescent solar concentrator module", Renewable Energy 76,
547 pp. 330-337.
- 548 [16] van Sark, W.G.J.H.M. 2013, "Luminescent solar concentrators - A low cost
549 photovoltaics alternative", Renewable Energy, vol. 49, pp. 207-210.
- 550 [17] Ugumori, T. & Ikeya, M. 1981, "Efficiency increase of solar cells operated in
551 dielectric liquid", Japanese Journal of Applied Physics, vol. 20, pp. 77-80.
- 552 [18] Wang, Y., Fang, Z., Zhu, L., Huang, Q., Zhang, Y. & Zhang, Z. 2009, "The
553 performance of silicon solar cells operated in liquids", Applied Energy, vol. 86, no. 7-8,
554 pp. 1037-1042.
- 555 [19] Han, X., Wang, Q. & Zheng, J. 2016, "Determination and evaluation of the optical
556 properties of dielectric liquids for concentrating photovoltaic immersion cooling
557 applications", Solar Energy, vol. 133, pp. 476-484.
- 558 [20] Vivar, M. & Everett, V. 2014, "A review of optical and thermal transfer fluids used
559 for optical adaptation or beam-splitting in concentrating solar systems", Progress in
560 Photovoltaics: Research and Applications, vol. 22, no. 6, pp. 612-633.
- 561 [21] NFPA. 2001, "Standard system for the identification of the hazards of materials for
562 emergency response NFPA-704", National Fire Protection Association.
- 563 [22] Stenzel, O. 2005, "The Physics of Thin Film Optical Spectra: An Introduction".
564 Springer, New York.
- 565 [23] Green, M.A. 1982, "Solar Cells", Prentice-Hall, Englewood Cliffs, NJ.
- 566 [24] Victoria, M., Askins, S., Domínguez, C., Antón, I. & Sala, G. 2013, "Durability of
567 dielectric fluids for concentrating photovoltaic systems", Solar Energy Materials and
568 Solar Cells, vol. 113, pp. 31-36.